Sensor Fusion for Glucose Monitoring Systems

Ahdab, Mohamad Al; Benam, Karim Davari ; Khoshamadi, Hasti ; Fougner, Anders Lyngvi ; Gros, Sebastien

Published in:
IFAC-PapersOnLine

DOI (link to publication from Publisher):
10.1016/j.ifacol.2023.10.444

Publication date:
2023

Document Version
Publisher's PDF, also known as Version of record

Sensor Fusion for Glucose Monitoring Systems ⋆

Mohamad Al Ahdab * **Karim Davari Benam** **
Hasti Khoshamadi ** **Anders Lyngvi Fougner** **
Sebastien Gros **

* *Section of Automation and Control, Department of Electronic Systems, Aalborg University, Aalborg Øst, Denmark, (e-mail:maah@es.aau.dk)*
** *Department of Engineering Cybernetics, Faculty of Information Technology and Electrical Engineering, Norwegian University of Science and Technology (NTNU), O. S. Bragstads Plass 2D, 7034 Trondheim, Norway (e-mail: {karim.d.benam, hasti.khoshamadi, anders.fougner, sebastien.gros}@ntnu.no)*

Abstract: A fully automated artificial pancreas (AP) requires accurate blood glucose (BG) readings. However, many factors can affect the accuracy of commercially available sensors. These factors include sensor artifacts due to the pressure on surrounding tissues, connection loss, and poor calibration. The AP may administer an incorrect insulin bolus due to inaccurate sensor data when the patient is not supervising the system. The situation can be even worse in animal experiments because animals are eager to play with the sensor and apply pressure.
In this study, we propose and derive a Multi-Model Kalman Filter with Forgetting Factor (MMKFF) for the problem of fusing information from redundant subcutaneous glucose sensors. The performance of the developed MMKFF was assessed by comparing it against other Kalman Filter (KF) strategies on experimental data obtained in two different animals. The developed MMKFF was shown to provide a reliable fused glucose reading. Additionally, compared to the other KF approaches, the MMKFF was shown to be better able to adjust to changes in the accuracy of the glucose sensors.

Keywords: Developments in measurement, signal processing, Diabetes.

1. INTRODUCTION

Monitoring blood glucose (BG) level in subjects with diabetes is important for managing their treatment. Over the last two decades, continuous glucose monitoring (CGM) systems have become more and more common in patients with diabetes mellitus type 1. Most commercially available CGMs provide measurement samples each 5 minutes allowing for a better description of the subject's glucose variability.

The artificial pancreas (AP) automates BG control by reading levels from a CGM, calculating the insulin bolus dose using a control algorithm, and infusing the insulin with a pump. A reliable system for measuring BG level with minimal supervision is essential to achieve the ultimate goal of reducing supervision. However, real-life situations can cause CGMs to provide inaccurate information or disconnect from APs, posing a risk to BG control in a single-sensor APs.

For simplicity and to reduce the wiring, the common off-the-shelf CGMs have a transmitter to connect wirelessly with the AP. The communication methods are Bluetooth or ANT+, which will lose connection if the CGM and the receiver/pump are on opposite sides of the body, e.g. during sleep. Furthermore, compression artifacts caused by external pressure on the CGM can rapidly decrease the measured BG level and cause failure of the APs. Many other circumstances make single-sensor APs unreliable, making the supervision of the CGM necessary for patients. These circumstances have been summarised by Facchinetti (2016).

The glucose sensors have a warm-up period, which means that each new sensor attached will not provide accurate data for a while. Warm-up times vary between brands and range from 2 hours to 2 days. In other words, if the CGM fails unexpectedly in single-sensor APs, patients must manually control the BG during the warm-up period of the new sensor. The issue gets aggravated in awake animal experiments since it is challenging to take frequent blood samples to measure the BG. Additionally, since animals are eager to play with the sensors attached to their bodies or exert pressure on them, the circumstances above are more likely to occur in animal experiments. Notably, the warm-up period in the animal experiment is not ideal because it lengthens the experiment and raises the cost of the experiment. In this setting, the animal experiments are used to test controllers.

Redundant sensors are advised in the literature to address the issues above. For example, Jacobs et al. (2014) used

⋆ This work was funded by the IFD Grand Solution project ADAPT-T2D, project number 9068-00056B, the Research Council of Norway (project no. 248872), and the Centre for Digital Life Norway.

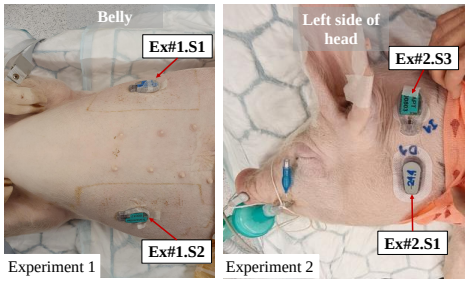

Fig. 1. Placement of glucose sensors. Left: Experiment 1, both sensors Exp1.S1 and Exp1.S2 placed on the pig's belly. Right: Experiment 2, two sensors on the left side of the neck. Another two sensors were on the pig's right side, with sensor Exp2.S4 attached at the bottom and Exp2.S2 at the top.

two sensors in their AP where one sensor would replace the active one in the event of a sensor failure. In the present study, instead of using the other sensor(s) only for backup, we developed a method based on a Multi-Model Kalman Filter (MMKF) approach to combine the data from all the glucose sensors attached on the subject to increase the reliability. The proposed method was evaluated using experimental data from anesthetized and awake pigs.

The works in Facchinetti et al. (2013, 2015); Vettoretti et al. (2019) used data batches from multiple CGMs devices together with an accurate reference BG data for the aim of obtaining a detailed parametric model description for the measurement errors in specific CGM devices. Therefore, the methods developed in these works are not suitable for a real time sensor fusion of CGMs for APs.

Kalman Filter (KF) strategies have been used in previously reported studies with CGMs for the purpose of calibrating one CGM device with self monitored blood glucose samples obtained by finger pricking Knobbe and Buckingham (2005); Kuure-Kinsey et al. (2006); Facchinetti et al. (2010). While these solutions primarily focused on sensor calibration, in this paper we aim to fuse information from numerous CGM devices with varying degrees of accuracy considering that one or more sensors can fail and recover over time.

The contributions of this work are as following:

- We show how MMKF can be used for the fusing of CGM devices. In addition, we derive a MMKF with a Forgetting Factor (MMKFF) in Section 4.
- We apply the MMKFF on two sets of experimental data and evaluate its performance in Section 5 comparing it with different types of KFs.

2. ANIMAL EXPERIMENTS

The example data sets used in this paper are from two different animal experiments. The tests were carried out in two non-diabetic farm pigs (Sus scrofa domesticus) of 36 and 40 kg, respectively.

The first experiment (Exp1) was performed in an anesthetized pig for 24 hours. Three Medtronic Enlite glucose sensors (Northridge, Canada) with custom transmitters from Inreda Diabetic (Goor, the Netherlands) were used (hereafter named Exp1.S1, Exp1.S2, and Exp1.S3) with a 1.2s sampling time. The provided data acquisition system could only receive data from two of the sensors. Therefore, one of the sensors only served as a backup sensor. Blood samples were taken sporadically to calibrate the sensors and compare them. A blood gas analyser (BGA) of ABL800 FLEX (Copenhagen, Denmark) was used to measure the actual BG level throughout the experiment. We compared the performance of the developed MMKFF method with the BGA. Exp1.S1 and Exp1.S2 were attached to each side of the belly as shown in Figure. 1, and Exp1.S3 was attached to the neck as backup. The protocol for this animal experiment was similar to the protocols used in Halvorsen et al. (2022) and Benam et al. (2023).

The second experiment (Exp2) was closer to real-life conditions than Exp1 since it was performed in an awake animal where it could move freely. In this experiment, four sensors were used to decrease the chance of losing data or basing decisions on faulty data. Sensors Exp2.S1 and Exp2.S2 were factory-calibrated Dexcom G6 (San Diego, CA) with 5min sampling time. Sensors Exp2.S3 and Exp2.S4 were Medtronic Guardian sensors 3 (Northridge, Canada) with custom-made transmitters from Inreda Diabetic (Goor, the Netherlands) with 1.2s sampling time. To reduce the connection losses during the experiments, the sensors were mounted on both sides of the neck, as shown in Figure 1. Unlike Exp1, taking frequent blood samples was not possible. However, depending on the sensor connection losses, general behaviours of the sensors compared to others, and position of the pig, the experiment's operators were giving each sensor a reliability indicator between 0 and 1. Then we calculated a weighted average of the sensors using their assigned reliability indicators. With the weighted average value as a benchmark, we evaluated the performance of the proposed sensor fusion technique. Readings at time $5k$ [min], $k \in \mathbb{Z}_{\geq 0}$ from Exp1.S1/ Exp2.S1, Exp1.S2/Exp2.S2, Exp2.S3, and Exp2.S4 will be denoted as $y_k[1]$,$y_k[2]$,$y_k[3]$, and $y_k[4]$, respectively.

3. NOTATIONS

For a random variable x, we write x for its realization. We write $\mathcal{N}(\mu, \Sigma)$ for the normal distribution with mean μ and variance Σ. Let two successive time instants t_k and t_{k+j} be such that $t_{k+j} - t_k = jT$, $j \in \mathbb{Z}$ with $T \in \mathbb{R}$, then variables $x(t_k), x(t_{k+j})$ will be denoted as x_k, x_{k+j}. The symbol $\mathbb{S}^n_{>0}$ ($\mathbb{S}^n_{\geq 0}$) is used for the set of positive definite (semi-definite) matrices with dimension n. We write $[N] = \{1, \ldots, N\}$, $N \in \mathbb{Z}_{>0}$. We write a diagonal matrix with diagonal elements $v = [v_1, \ldots, v_n]^\top$ as $\mathrm{diag}\,(v)$. We use $\mathbf{I}$ for the identity matrix.

4. METHOD

In this section, we will first present the models used for the glucose sensors in 4.1. Afterwards, the MMKFF method will be described in 4.2.

4.1 Problem Setup

We consider a setup in which we have $N \in \mathbb{Z}_{>0}$ CGM sensors. At each sample time k, a portion of the sensors

$0 \leq n_k \leq N$ will provide readings $y_k \in \mathbb{R}^{n_k}$. This setup considers cases when the sensors can fail for some periods of time. For the modeling, we consider in this paper N linear Gaussian dynamic models $\mathcal{M}^i$ with $i \in [N]$ as the following

$$x^i_{k+1} = A^i x^i_k + E^i w^i_k,\ w^i_k \sim \mathcal{N}(0, Q^i), \tag{1a}$$

$$y_k = C^i_k x^i_k + v^i_k,\ v^i_k \sim \mathcal{N}(0, R^i_k), \tag{1b}$$

with $x^i \in \mathbb{R}^{n_x}, n_x \in \mathbb{Z}_{>0}$, $A^i \in \mathbb{R}^{n_x \times n_x}$, $E^i \in \mathbb{R}^{n_x \times n_q}$, $n_q \in \mathbb{Z}_{>0}$, $Q_i \in \mathbb{S}^{n_q}_{>0}$, w^i_k is an independent and identically distributed (IID) process, $C^i_k \in \mathbb{R}^{n_k \times n_x}$, $R^i_k \in \mathbb{S}^{n_k}_{\geq 0}$, and $v^i_k \in \mathbb{R}^{n_k}$ is a IID process. Similar to the previous works in Knobbe and Buckingham (2005); Facchinetti et al. (2010) in which integrators of white noise with different orders are chosen to represent a description for the dynamics of BG concentrations, we choose matrices $A^i = A,\ E^i = E,\ Q^i = Q$ and $C^i_k = C_k$ for all the models $i \in [N]$ such that A, E, Q, and C represent the discrete output of a triple integrated white noise w as following

$$A = \begin{bmatrix} 1 & 0 & 0 \\ T & 1 & 0 \\ T^2/2 & T^3/6 & 1 \end{bmatrix}, E = \begin{bmatrix} T \\ T^2/2 \\ T^3/6 \end{bmatrix}, C_k = \begin{bmatrix} 0 & 0 & 1 \\ & \vdots & \\ 0 & 0 & 1 \end{bmatrix} \in \mathbb{R}^{n_k \times 3},$$

with T [min] being the sampling time [1]. The integrated white noise model serves as a prior assumption regarding the stationarity and the power spectrum density of the BG concentration. Additionally, if the model in (1a) is viewed as a discretized version of a continuous time dynamical glucose model, then it captures our knowledge that BG concentration is differentiable with respect to time. This choice is common in time series estimation of physiological processes (see De Nicolao et al. (1997) for e.g.). The higher the order of the integrator, the smoother the continuous time BG concentration is assumed to be. The variance Q of the driving white noise can be understood as a representation of how confident we are in the assumed model (see Section 5.1 for more details). Note that the model does not reflect the ground truth of the time evolution for BG concentration and different models with different accuracy and inputs (e.g. insulin, physical activity, meals, etc...) can also be considered and used. For the simplicity in this paper, we considered a simple white noise integrator which can work in a general setting in which data regarding more specific inputs is not available. As for the covariance matrix R^i_k for the measurement noise, it will be chosen differently for each model $i \in [N]$. To define R^i_k, let $r^i \in \mathbb{R}^N$ such that the i_{th} element of r^i is σ^2_l while the rest of the elements in r^i are σ^2_u with $\sigma_u > \sigma_l$. Let $s_k \in \mathbb{R}^N$ such that the i_{th} element of s_k is 1 if the i_{th} sensor is providing a reading at sample k and zero otherwise. Then the covariance matrix R^i_k is chosen as $R^i_k = \text{diag}\left(s^\top_k r^i\right)$. This basically means that for each sensor i, we have a model $\mathcal{M}^i$ that assumes a lower variance for the i_{th} sensor (σ^2_l) than the variance for the other sensors (σ^2_u). In other words, each model is more confident with respect to one sensor than the others. Note that it is possible with this structure to have a continuum of models weighting the sensors differently. However, we chose to have a finite number of models for simplicity and tractability. Finally, we define for each model $\mathcal{M}^i$ a random variable $m^i_k \in \{0, 1\}$ such that $p(\text{m}^i) = \mathbb{P}(\text{m}^i_k = 1) := \mathbb{P}\left(\mathcal{M}^i \text{ is the best model at step } k\right)$. Note that the time dependence for m^i_k is included to account for the fact that some sensors will become better than others for a period of time. To relate m^i_{k+1} with m^i_k, we use the following

$$p(\text{m}^i_{k+1}) = p(\text{m}^i_{k+1}|\text{m}^i_k)p(\text{m}^i_k) := (1-\alpha)p(\text{m}^i_k) + \alpha\bar{\beta}^i, \tag{2}$$

with $0 \leq \alpha \leq 1$ a constant which we call the *forgetting factor*, and $0 \leq \bar{\beta}^i \leq 1$ with $\sum_{i=1}^N \bar{\beta}^i = 1$ are predefined probabilities for the models. The dynamic model in (2) is to be understood as a prior model in the absence of measurement updates (similar to (1a)). A measurement correction step will be introduced in section 4.2. To understand more what "forgetting" is meant with (2), assume we start from probabilities $p(\text{m}^i_k) > 0,\ \forall i \in [N]$ representing our knowledge at step k regarding the models. If we only follow the update in equation (2), then the $l - step$ prediction is $p(\text{m}^i_{k+l}) = (1-\alpha)^l p(\text{m}^i_k) + \left(1 - (1-\alpha)^l\right)\bar{\beta}^i$. If $0 < \alpha \leq 1$, we can see that $\lim_{l\to\infty} p(\text{m}^i_{k+l}) = \bar{\beta}^i$. This means that $\forall i \in [N]$, our knowledge regarding the models $p(\text{m}^i_k)$ with equation (2) only is "forgotten" exponentially with a rate $1 - \alpha$ to converge to a predefined knowledge captured in $\bar{\beta}^i$. The predefined probabilities $\bar{\beta}^i$ can be uniform ($\bar{\beta}^i = \frac{1}{N},\ \forall i \in [N]$) or prior probabilities regarding the models.

4.2 Multiple Models Kalman Filter with Forgetting Factor

The idea of the MMKF, which was first introduced in Magill (1965), is to run a KF for each model $\mathcal{M}^i$ in parallel and combine the estimated results to obtain a better new estimate. In this section, we will extend the MMKF with the forgetting factor equation (2) and provide a description for the MMKFF strategy. Note that the MMKFF can be thought of as a specific case for dynamic MMKF where the probabilities of the true models evolve with time and it is different from the one in (Bar-Shalom et al., 2004, chapter 11) since (7) is not a homogeneous Markov chain. For ease of notation, we will use $\beta^i_{k_1|k_2} := p\left(\text{m}^i_{k_1}|\mathcal{Y}_{k_2}\right)$ with $k_1, k_2 \in \mathbb{Z}_{\geq 0}$, and $\mathcal{Y}_{k_2} = (y_1, \ldots, y_{k_2})$ being a tuple of all the available measurement up until sample k_2. Assume now at iteration k we have an estimate $\hat{x}_{k|k} \sim \mathcal{N}\left(\mu_{k|k}, P_{k|k}\right)$ for the states and probabilities $\beta^i_{k|k}$. If there is an available measurement reading y_{k+1}, then we run a KF for each model $\mathcal{M}^i$ as following

Time update:

$$\mu_{k+1|k} = A\mu_{k|k}, P_{k+1|k} = AP_{k|k}A^\top + EQE^\top \tag{3a}$$

Measurement Correction:

$$\tilde{y}_{k+1|k} = y_{k+1} - C_k\mu_{k+1|k},\ S^i_{k+1|k} = C_k P^i_{k+1|k} C^\top_k + R^i_k \tag{4a}$$

$$\mu^i_{k+1|k+1} = \mu_{k+1|k} + P_{k+1|k}C^\top_k (S^i_{k+1|k})^{-1}\tilde{y}_{k+1|k} \tag{4b}$$

$$P^i_{k+1|k+1} = \left(\mathbf{I} - P_{k+1|k}C^\top_k (S^i_{k+1|k})^{-1}C_k\right) P_{k+1|k} \tag{4c}$$

To derive a time update step and a measurement correction step for the probabilities $\beta^i_{k+1|k+1}$, we use Baye's rule to write

$$\beta^i_{k+1|k+1} = p(\text{m}^i_{k+1}|\mathcal{Y}_{k+1}) = \frac{p(\text{m}^i_{k+1}, \mathcal{Y}_{k+1})}{p(\mathcal{Y}_{k+1})}$$

[1] If the sensors are operating at different sampling rates then T can be chosen to be the minimum of the different sampling times.

$$
\begin{aligned}
&= \frac{p(\mathrm{m}^i_{k+1}, \mathcal{Y}_k, \mathrm{y}_{k+1})}{p(\mathcal{Y}_{k+1})} = \frac{p(\mathrm{m}^i_{k+1}, \mathcal{Y}_k, \tilde{\mathrm{y}}_{k+1|k})}{p(\mathcal{Y}_{k+1})} \\
&= \frac{p(\tilde{\mathrm{y}}_{k+1|k}|\mathrm{m}^i_{k+1}, \mathcal{Y}_k)p(\mathrm{m}^i_{k+1}, \mathcal{Y}_k)}{p(\mathcal{Y}_{k+1})} \\
&= \frac{p(\tilde{\mathrm{y}}_{k+1|k}|\mathrm{m}^i_{k+1})p(\mathrm{m}^i_{k+1}|\mathcal{Y}_k)p(\mathcal{Y}_k)}{p(\mathcal{Y}_{k+1})} \\
&= \frac{p(\tilde{\mathrm{y}}_{k+1|k}|\mathrm{m}^i_{k+1})p(\mathrm{m}^i_{k+1}|\mathcal{Y}_k)}{p(\tilde{\mathrm{y}})} \\
&= \frac{p(\tilde{\mathrm{y}}_{k+1|k}|\mathrm{m}^i_{k+1})}{\sum_{i=1}^N p(\tilde{\mathrm{y}}_{k+1|k}|\mathrm{m}^i_{k+1})p(\mathrm{m}^i_{k+1}|\mathcal{Y}_k)} p(\mathrm{m}^i_{k+1}|\mathcal{Y}_k)
\end{aligned} \tag{5}
$$

with

$$
\begin{aligned}
p(\mathrm{m}^i_{k+1}|\mathcal{Y}_k) &= p(\mathrm{m}^i_{k+1}|\mathrm{m}^i_k)p(\mathrm{m}^i_k|\mathcal{Y}_k) \\
&= (1-\alpha)p(\mathrm{m}^i_k|\mathcal{Y}_k) + \alpha\bar{\beta}^i
\end{aligned} \tag{6}
$$

To summarize, (5) and (6) are written as a time update step and a measurement correction step with the notation $\beta^i_{k_1|k_2}$ as following

Time update (using (6)):

$$
\beta^i_{k+1|k} = (1-\alpha)\beta^i_{k|k} + \alpha\bar{\beta}^i \tag{7}
$$

Measurement Correction (using (5)):

$$
\beta^i_{k+1|k+1} = \frac{p\left(\tilde{y}_{k+1|k} \mid \mathrm{m}^i_{k+1}\right)}{\sum_{i=1}^N \beta^i_{k+1|k} p\left(\tilde{y}_{k+1|k} \mid \mathrm{m}^{\mathrm{i}}_{\mathrm{k+1}}\right)} \beta^i_{k+1|k}. \tag{8}
$$

with $p\left(\tilde{y}_{k+1|k} \mid \mathrm{m}^i_{k+1}\right)$ being the multi-normal probability density function with zero mean and covariance matrix $S^i_{k+1|k}$. Finally, let $\Delta\mu^i_{k+1} := \mu^i_{k+1|k+1} - \mu_{k+1|k+1}$, then the estimated mean and covariance matrix of the states are computed as following

$$
\mu_{k+1|k+1} = \sum_{i=1}^N \beta^i_{k+1|k+1}\mu^i_{k+1|k+1} \tag{9a}
$$

$$
P_{k+1|k+1} = \sum_{i=1}^N \beta^i_{k+1|k+1}\left(P^i_{k+1|k+1} + \Delta\mu^i_{k+1}\left(\Delta\mu^i_{k+1}\right)^\top\right). \tag{9b}
$$

Note that the values $\beta^i_{k+1|k+1}$ in (9a) are acting as weights for the estimates obtained from the different KFs. The values $\beta^i_{k+1|k+1}$ will be referred to as "trust values for sensor i" in the next section.

5. RESULTS

We compare the MMKFF presented in this paper with the following KFs:

- Linear KF.
- The Distributionally Robust KF (DRKF) from Wang and Ye (2022) with a moment based ambiguity set and an $\epsilon-$contamination set for outliers.
- The Adaptive Fading KF (AFKF) based on Xia et al. (1994) but with the fading applied to the covariance matrix $R(k)$ adapting to sensor changes.
- The MMKF.

5.1 Choice of the Kalman Filters' Parameters

All the KFs share the same value of Q. For a higher value of Q, the KFs will rely on the measurements more for their estimates which will make them faster to respond to changes in BG but more prone to noise. On the other hand, a smaller value of Q will make the KFs rely more on the model predictions but will hinder their ability to respond quickly to changes in BG. The value of Q in this paper was chosen to be $Q = 1$. For the distributionally robust KF, we tuned the parameters denoted in the paper Wang and Ye (2022) as $\theta_{2,x}, \theta_{2,v}, \epsilon$ to be $\theta_{2,x} = \theta_{2,v} = 1.02$ and $\epsilon = 0.005$. For Exp1, we only compared MMKF and MMKFF due to limited space. For Exp2, the one model KFs share one covariance matrix $R_k = \mathrm{diag}\left(s_k^\top r\right)$ with $r = [1\ 1\ 100\ 100]^\top$ since our prior knowledge is such that Exp2.S1 and Exp2.S2 perform better than Exp2.S3 and Exp2.S4. For the multi-model KFs, we chose $\sigma_l^2 = 1$ and $\sigma_u^2 = 100$ for the both experiments. The forgetting factor was chosen to be $\alpha = 0.05$. The KFs for both Exp1 and Exp2 were initialized with $\mu_{0|0} = [0\ 0\ 0.5y_0[1] - 0.5y_0[2]]^\top$ and $P_{0|0} = \mathbf{I}$ where $y_0[1]$ and $y_0[2]$ are the measurements of the first and second sensors of both experiments, respectively. For Exp1, we chose $\beta_{0|0} = \bar{\beta} = [0.5\ 0.5]^\top$ based on our prior knowledge (no prior preference over the sensors). As for Exp2, $\beta_{0|0} = \bar{\beta} = [0.3\ 0.3\ 0.2\ 0.2]^\top$ based on our prior knowledge.

5.2 Results from Exp1

In Figure 2, MMKFF and MMKF were tested on data from Exp1.S1 and Exp2.S2 and the result compared to BGA. The MMKF and MMKFF performed similarly, with their fused CGM being close to the accurate BG readings. The fused CGM managed to overcome the drifting in Exp1.S2 and stayed close to the reading from the Blood Gas Analyser (BGA). However, we can see that the trust values $\beta^1_{k|k}$ and $\beta^2_{k|k}$ evolved differently with the CGM readings. The trust values from the MMKF converged faster towards Exp1.S1 ($\beta^1_{k|k} \approx 1$, $\beta^2_{k|k} \approx 0$) during the case when Exp1.S2 was being calibrated than the trust values of MMKFF (see Figure 3). In this particular excerpt for Exp1, favoring Exp1.S1 quickly from the beginning as done by MMKF is better since the performance of Exp1.S2 continued to degrade during the period of data collection. However, events like Exp2.S2 improving beyond the calibration point without drifting or Exp1.S1 deteriorating during the trial, for instance, due to connection loss, can still occur. In these events, the MMKFF will perform better than MMKF since it does not immediately converge to trusting one sensor over the others. Additionally, it is able to "forget" past experiences which will enable it to adapt to new changes. This is shown in the findings for Exp2, where the MMKFF outperformed the MMKF in a more realistic case where the quality of the sensors varied over time. It is important to note that even though forgetting can offer better adaptivity to changes in the quality of sensors, it comes with the cost of slower reaction towards abrupt events as seen in Figure 3. The lower the forgetting factor, the faster the reaction of MMKFF to abrupt events and vice versa.

5.3 Results from Exp2

Figure 4 shows the results for three different excerpts of Exp2 compared to a fused CGM signal obtained by

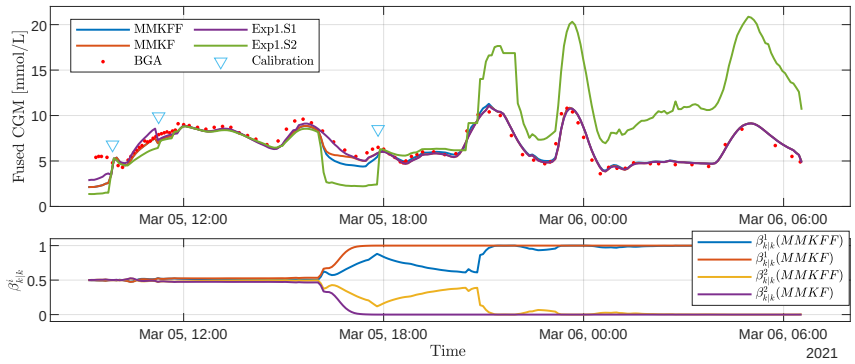

Fig. 2. Results from Exp1. BGA represents the values from the blood gas analyser, and 'Calibration' represents points where sensors S1 and S2 were calibrated using the BGA values. The Upper plot shows a comparison between MMKFF and MMKF using the readings from Exp1.S1 and Exp1.S2, while the lower plot shows the trust values β^i in (8) for each of the sensors $i \in \{1, 2\}$.

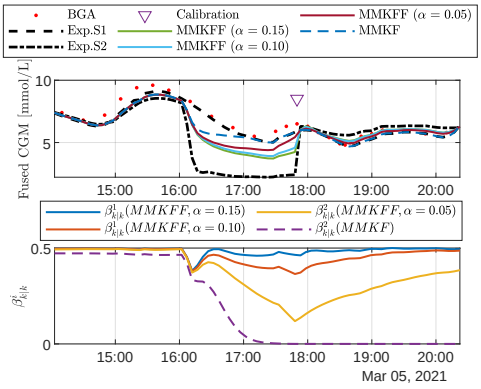

Fig. 3. The upper plot shows the response of MMKFF and MMKF with different forgetting factors, while the lower plot shows the trust values.

manually tuning a weighted average of the four CGMs in an online fashion (labeled Manual in the plots). In the first excerpt (left of the figure), the four sensors were all working as expected and readings were provided each 5 minutes. The MMKFF was the closest to the manually tuned signal. For the second excerpt (middle of the figure), Exp2.S3 was not working properly and stopped providing measurements towards the end. Additionally, Exp2.S2 was performing poorly with missing measurements and reporting readings which were close to 0 [mmol/L] while Exp2.S4 was performing better and close to Exp2.S1. This situation is challenging not only due to the missing and wrong readings of some sensors, but also due to the fact that our prior knowledge prefers Exp2.S1 and Exp2.S2 over Exp2.S3 and Exp2.S4. Despite these challenges, the MMKFF performed the best in the sense of being the closest to the manually tuned reading. Observe how both the MMKF and MMKFF reduced the trust value of Exp2.S4 when it stopped providing readings around 50 [min] of the excerpt. However, the MMKFF increased the trust value of Exp2.S4 when it started providing good readings again, unlike the MMKF. Moreover, the MMKFF started trusting Exp2.S2 more when its readings improved. For the third excerpt (right of the figure), Exp2.S3 was not providing any readings, and Exp2.S4 started providing readings around the time when Exp2.S1 and Exp2.S2 stopped providing readings. Out of the four KFs, the MMKFF was still the closest to the manually tuned reading on average and had the lowest maximum ARE value. Additionally, notice how it was difficult for the MMKF to increase its trust value of EX2.S4 again when it was providing readings. On the other hand, the MMKFF increased the trust value of EX2.S4 when it started providing readings again. These results show how the MMKFF is able to adapt better to changes in the quality of the sensors.

6. CONCLUSION AND FUTURE WORK

For CGM devices, the MMKFF fusing approach was introduced. The technique was evaluated using two separate sets of experimental data, and it was shown to be capable of producing a reliable fused CGM signal. It was demonstrated that MMKFF can respond to variations in the quality of the CGM readings more effectively when compared to other KF approaches. However, it was observed that MMKFF's ability for adaptation came at the expense of a slower reaction to sudden changes. Future studies could improve this by taking into account an adaptive forgetting factor for MMKFF. Additionally, the past data and inputs can be used with the high gain observer suggested in Benam et al. (2019) and Benam et al. (2022) to estimate the BG levels when the sensor connection is lost. Evaluating the proposed fusing approach on additional data from various experiments can provide a better understanding of the strategy's performance and its likelihood of being applied in a human environment.

7. ACKNOWLEDGMENT

The experimental services were provided by the Comparative medicine Core Facility (CoMed), Norwegian University of Science and Technology (NTNU). CoMed is funded by the Faculty of Medicine at NTNU and Central Norway Regional Health Authority. The transmitters (for Exp1 and Exp2) and the hormone infusion systems in Exp1 were provided by Inreda Diabetic BV (Goor, the Netherlands). We want to thank Marte Kierulf Åm, Oddveig Lyng, and Patrick Christian Bösch for their invaluable contribution to the data collection. We also thank Professor Sven Magnus Carlsen for his help in experimental design and discussions.

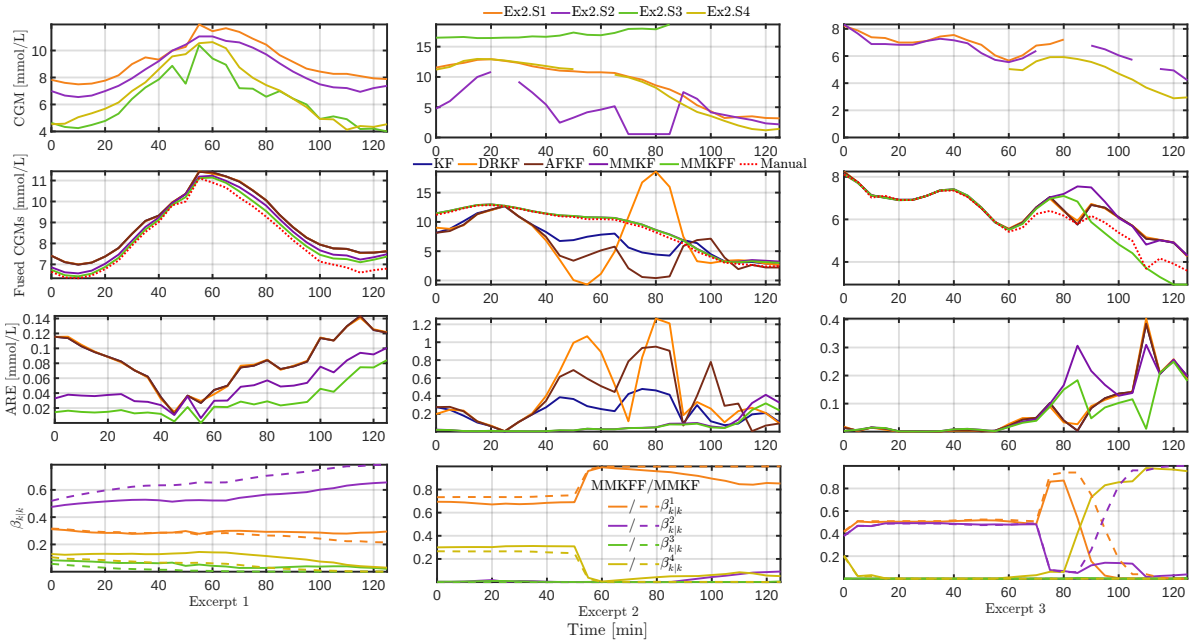

Fig. 4. Results of fusion using four different glucose sensors in the Exp2, for three different excerpts (left, middle, right column). First row: Original glucose sensor values for sensors S1 to S4. Second row: Comparison of fused glucose sensor values for the various sensor fusion methods. Third row: ARE (absolute relative error with respect to manual sensor fusion). Fourth row: Trust values $\beta^i_{k|k}$ in (8), where solid lines are MMKFF and dashed lines are MMKF.

REFERENCES

Bar-Shalom, Y., Li, X.R., and Kirubarajan, T. (2004). *Estimation with applications to tracking and navigation: theory algorithms and software*. John Wiley & Sons.

Benam, K.D., Khoshamadi, H., Åm, M.K., Stavdahl, Ø., Gros, S., and Fougner, A.L. (2023). Identifiable prediction animal model for the bi-hormonal intraperitoneal artificial pancreas. *Journal of Process Control*, 121, 13–29.

Benam, K.D., Khoshamadi, H., Lema-Pérez, L., Gros, S., and Fougner, A.L. (2022). A nonlinear state observer for the bi-hormonal intraperitoneal artificial pancreas. In *2022 44th Annual International Conference of the IEEE Engineering in Medicine & Biology Society (EMBC)*, 171–176. IEEE.

Benam, K.D., Talebi, H., and Khosravi, M.A. (2019). Full order high gain observer design for image-guided robotic flexible needle steering. In *2019 27th Iranian Conference on Electrical Engineering (ICEE)*, 1151–1156. IEEE.

De Nicolao, G., Sparacino, G., and Cobelli, C. (1997). Nonparametric input estimation in physiological systems: Problems, methods, and case studies. *Automatica*, 33(5), 851–870.

Facchinetti, A. (2016). Continuous glucose monitoring sensors: past, present and future algorithmic challenges. *Sensors*, 16(12), 2093.

Facchinetti, A., Del Favero, S., Sparacino, G., et al. (2013). Modeling the glucose sensor error. *IEEE Trans Biomed Eng*, 61(3), 620–629.

Facchinetti, A., Del Favero, S., Sparacino, G., et al. (2015). Model of glucose sensor error components: identification and assessment for new dexcom g4 generation devices. *Medical & biological engineering & computing*, 53(12), 1259–1269.

Facchinetti, A., Sparacino, G., and Cobelli, C. (2010). Enhanced accuracy of continuous glucose monitoring by online extended kalman filtering. *Diabetes technology & therapeutics*, 12(5), 353–363.

Halvorsen, M., Benam, K.D., Khoshamadi, H., and Fougner, A.L. (2022). Blood glucose level prediction using subcutaneous sensors for in vivo study: Compensation for measurement method slow dynamics using kalman filter approach. In *2022 IEEE 61st Conference on Decision and Control (CDC)*, 6034–6039. IEEE.

Jacobs, P.G., El Youssef, J., Castle, J., et al. (2014). Automated control of an adaptive bihormonal, dual-sensor artificial pancreas and evaluation during inpatient studies. *IEEE Trans Biomed Eng*, 61(10), 2569–2581.

Knobbe, E.J. and Buckingham, B. (2005). The extended kalman filter for continuous glucose monitoring. *Diabetes technology & therapeutics*, 7(1), 15–27.

Kuure-Kinsey, M., Palerm, C.C., and Bequette, B.W. (2006). A dual-rate kalman filter for continuous glucose monitoring. In *2006 Int Conf of the IEEE Engineering in Medicine and Biology Society*, 63–66. IEEE.

Magill, D. (1965). Optimal adaptive estimation of sampled stochastic processes. *IEEE Transactions on Automatic Control*, 10(4), 434–439.

Vettoretti, M., Battocchio, C., Sparacino, G., et al. (2019). Development of an error model for a factory-calibrated continuous glucose monitoring sensor with 10-day lifetime. *Sensors*, 19(23), 5320.

Wang, S. and Ye, Z.S. (2022). Distributionally robust state estimation for linear systems subject to uncertainty and outlier. *IEEE Transactions on Signal Processing*, 70, 452–467.

Xia, Q., Rao, M., Ying, Y., and Shen, X. (1994). Adaptive fading kalman filter with an application. *Automatica*, 30(8), 1333–1338.